Comparative Evaluation of Capsular Polysaccharide-Specific IgM and IgG Antibodies and F(ab′)$_2$ and Fab Fragments as Delivery Vehicles for Radioimmunotherapy of Fungal Infection

Ekaterina Dadachova,[1,2] Ruth A. Bryan,[1] Xianchun Huang,[1] Geraldina Ortiz,[1] Tiffany Moadel,[1] and Arturo Casadevall[2]

Abstract

Purpose: The applicability of radioimmunotherapy with organism-specific monoclonal antibodies to treatment of infectious disease in experimental models has been recently shown for fungal, bacterial, and viral infections. To identify the best delivery vehicle for radioimmunotherapy of human pathogenic fungus *Cryptococcus neoformans* (CN), we have done comparative evaluation of capsular polysaccharide-specific antibodies with IgG1 and IgM isotypes and F(ab′)$_2$ and Fab fragments.

Experimental Design: 18B7 IgG1 and 13F1 IgM and their isotype-matching controls were radiolabeled with ^{188}Re, and their binding to 24067 and H99 CN strains was evaluated by doing Scatchard and kinetics analyses. The doses delivered during *in vitro* radioimmunotherapy were estimated using a cellular dosimetry algorithm. The biodistribution of ^{188}Re-labeled 18B7 and 13F1 and of ^{111}In-labeled 18B7 and its F(ab′)$_2$ and Fab fragments was done in A/JCr mice systemically infected with 24067 CN strain.

Results: 18B7 IgG1 showed superior to 13F1 IgM binding to 24067 CN ($K_a = 1.7 \times 10^9$ mol/L^{-1} and 5.4×10^7 mol/L^{-1}, respectively). Substantial killing of 24067 and H99 CN cells was achieved with 1 μCi ^{188}Re-18B7 (55 cGy dose), whereas no killing was observed for 1 μCi ^{188}Re-13F1 (2 cGy dose). *In vivo* ^{188}Re-18B7 localized specifically in the lungs of CN-infected mice, whereas uptake of ^{188}Re-13F1 was nonspecific. ^{111}In-F(ab′)$_2$ fragments showed higher uptake in the lungs and lower in the liver at the 48-h time point in comparison with intact ^{111}In-18B7.

Conclusions: Comparative evaluation of IgG and IgM and of F(ab′)$_2$ and Fab fragments as potential delivery vehicles for radioimmunotherapy of cryptococcal infection strongly suggests that affinity for the target antigen is an important prerequisite for successful targeting of infection *in vivo* and that *in vitro* affinity measurements may predict the *in vivo* efficacy of candidate monoclonal antibodies.

Current antimicrobial therapies are relatively inefficient in immunosuppressed patients, such as cancer patients or HIV-infected individuals. This problem combined with an increasing prevalence of diseases caused by highly resistant microorganisms creates an urgent need for new approaches to treatment of infectious diseases. Passive antibody therapy is a potentially useful therapeutic and preventive strategy against a variety of infectious diseases (1). The specificity of the antigen-antibody interaction provides an attractive option for delivering microbicidal agents to sites of infection. Recently, we showed the feasibility of radioimmunotherapy as an anti-infective therapy by treating murine cryptococcosis with a monoclonal antibody (mAb) to the *Cryptococcus neoformans* (CN) capsular glucuronoxylomannan labeled with 213-bismuth (^{213}Bi) or 188-rhenium (^{188}Re; refs. 2, 3). Subsequently, we showed the applicability of radioimmunotherapy to other fungal and bacterial infections (4, 5). Radioimmunotherapy also proved to be effective both *in vitro* and *in vivo* against HIV-1 chronically or acutely infected human cells (6).

The use of radioimmunotherapy for tumor therapy has been studied for 2 decades and there is a wealth of knowledge derived from both laboratory and clinical studies about the delivery of radionuclides by mAbs and their fragments, both murine and humanized, to cancer cells, surrounding tissue, and major organs (7, 8). In contrast, the application of radioimmunotherapy to infectious diseases is in its infancy, with experience limited to animal models. Most of the information on the issues associated with the application of mAbs as delivery vehicles for radioimmunotherapy of infectious diseases has been inferred from the literature on radioimmunotherapy of cancer as well as from the reports on the use of microorganism-specific mAbs for

Authors' Affiliations: Departments of [1]Nuclear Medicine and [2]Microbiology and Immunology, Albert Einstein College of Medicine, Bronx, New York

Received 4/13/07; accepted 5/16/07.

Grant support: National Institute of Allergy and Infectious Diseases grants AI52042 and AI60507 and Fighting Children's Cancers Foundation (E. Dadachova, A. Casadevall, R.A. Bryan, and X. Huang) and National Institute of Allergy and Infectious Diseases grants AI033142, AI033774, and HL059842 (A. Casadevall).

Presented at the Eleventh Conference on Cancer Therapy with Antibodies and Immunoconjugates, Parsippany, New Jersey, USA, October 12-14, 2006.

Requests for reprints: Ekaterina Dadachova, Department of Nuclear Medicine, Albert Einstein College of Medicine, 1695A Eastchester Road, Bronx, NY 10461. Phone: 718-405-8485; Fax: 718-405-8457; E-mail: edadacho@aecom.yu.edu.

doi:10.1158/1078-0432.CCR-07-0870

scintigraphic imaging of infection. Although some of this information is applicable to the development of radioimmunotherapy as an anti-infective modality, fundamental differences between neoplastic and infectious processes necessitate different approaches and considerations.

As a part of an on-going effort to translate the radioimmunotherapy of infection to the clinic, we have carried out a comparative evaluation of capsular polysaccharide-specific antibodies with IgG1 and IgM isotypes as well as of $F(ab')_2$ and Fab fragments as potential delivery vehicles for radioimmunotherapy of the human pathogenic fungus CN.

Materials and Methods

Cryptococcus neoformans. CN strains H99 (*C. neoformans var. grubii*) and 24067 (*C. neoformans var. neoformans*) were obtained from Dr. John Perfect (Duke University, Durham, NC) and the American Type Culture Collection, respectively. These two strains were chosen because of their clinical relevance as representative of the most common serotypes encountered in clinical practice in temperate regions. The cells were grown as in ref. 9.

CN-specific mAbs, fragments, and radiolabeling of mAb. Glucuronoxylomannan-binding murine mAb 18B7 (IgG1) and 13F1 (IgM) were produced as in refs. 10, 11. Isotype-matching control mAb MOPC21 (IgG1) and TEPC (IgM) were acquired from MP Biochemicals. $F(ab')_2$ and Fab fragments of 18B7 mAb were obtained by digestion using immobilized ficin from a commercial kit [ImmunoPure IgG1 Fab and $F(ab')_2$ preparation kit, Pierce]. Fab fragments were obtained by digestion of 18B7 for 3 h at 37°C on a ficin column in the presence of 20 mg/mL cysteine. $F(ab')_2$ fragments were prepared by digestion of 18B7 on the ficin column for 24 h at 37°C in the presence of 2 mg/mL cysteine. Following the digestions, the fragments were eluted from the column and purified by passage over a column of immobilized protein A to remove any components that contained the Fc portion of the antibody. The molecular weight of the obtained fragments was analyzed by SDS-PAGE and fast protein liquid chromatography. The protein concentration was determined by the method of Lowry et al. (12) using a kit from Bio-Rad. ^{111}In was purchased from Isotex; ^{188}Re was eluted from ^{188}Re/^{188}W generator (Oak Ridge National Laboratory). Whole IgG and IgM mAbs were radiolabeled with ^{188}Re "directly " as described (2). For radiolabeling of whole 18B7 and of its $F(ab')_2$ and Fab fragments with ^{111}In, the antibodies were incubated overnight at room temperature in bicarbonate buffer at pH 8.5 with 1.5 molar excess of bifunctional chelating agent *N*-[2-amino-3-(*p*-isothiocyanatophenyl)propy1]-*trans*-cyclohexane-1,2-diamine-*N,N′,N″,N‴,N⁗*-pentaacetic acid (CHXA"). Before incubation with CHXA", the thiol groups on Fab were blocked by the addition of 22 mmol/L iodoacetamide. The average number of CHXA" molecules per antibody was determined to be 1.0 to 1.5 by the Yttrium-Arsenazo III spectrophotometric method (13). The antibodies were purified from excess CHXA" on Centricon microconcentrators and radiolabeled with ^{111}In as in ref. 2.

Binding of mAbs 18B7 and 13F1 to H99 and 24067 cells. ^{188}Re-18B7 was added in different amounts to 24067 or H99 cells (2×10^6 per tube). After incubation for 1 h at 37°C, the tubes were counted in a gamma counter, the cells were collected by centrifugation, and the pellets were counted again. Scatchard analysis was used to compute the mAb binding constant and binding sites per cell as in ref. 14. In a separate series of experiments, the kinetics of mAbs 18B7 and 13F1 binding to 24067 cells was assessed. For this purpose, aliquots of cell suspension were removed after 0-, 10-, 20-, and 30-min and 1-h incubation time and centrifuged to separate the cell pellet from the supernatant, and the cell pellets were counted in a gamma counter.

In vitro *activity of ^{188}Re-labeled 18B7 and 13F1 against CN.* CN (10^5 cells) of 24067 and H99 strains was placed in microcentrifuge tubes in 0.1 mL PBS. Serially diluted ^{188}Re-18B7 or ^{188}Re-13F1 in 0.5 mL PBS was added to obtain the desired concentrations of radioactivity. After 60 min of incubation at 37°C, CN cells were collected by centrifugation, washed with PBS to remove nonbound radioactivity, suspended in 1 mL PBS, and incubated at 4°C for 48 h on a rocker. The cells did not divide during the incubation and maintenance periods because they were maintained in PBS, which lacks nutrients. Following the incubation, 10^3 cells were removed from each tube, diluted with PBS, and plated to determine colony-forming units (1 colony = 1 colony-forming unit). Experiments were done in duplicate.

Cellular dosimetry. To compare the doses delivered by ^{188}Re-labeled 18B7 and 13F1 to CN cells during radioimmunotherapy experiments, we used algorithm that we developed for radioimmunotherapy of fungal cells (4). Briefly, in this approach, the mean absorbed dose to the cell from cellular radioactivity is given by the following equation:

$$D_c = \tilde{A}\Sigma\, b_j\, S_j\ (C \leftarrow CS)$$

where $\tilde{A}$ is the cellular cumulated activity, bj is the branching ratio of the jth radionuclide in the decay series, and Sj(C←CS) is the cellular S value (absorbed dose to the cell per unit cumulated activity) for the jth radionuclide localized on the cell surface (CS) of the cell (C). The cumulated activity $\tilde{A}$ can be written as $\tilde{A} = \tilde{A}_I + \tilde{A}_M + \tilde{A}_{CF}$, where $\tilde{A}_I$, $\tilde{A}_M$, and $\tilde{A}_{CF}$ are the cellular cumulated activities during the periods of incubation for cellular uptake of radioactivity, maintenance at 4°C, and colony formation, respectively.

Biodistribution and scintigraphic imaging of ^{188}Re- and ^{111}In-labeled mAbs and fragments in A/JCr mice systemically infected with CN. All animal experiments were carried out in accordance with the guidelines of the Albert Einstein College of Medicine Institute for Animal Studies. In the first series of experiments, we did biodistribution measurements of ^{188}Re-18B7 IgG1 and ^{188}Re-13F1 IgM and of their respective isotype-matching controls ^{188}Re-MOPC21 and ^{188}Re-TEPC. Twelve groups of four A/JCr female mice (National Cancer Institute, Frederick, MD) were infected i.v. with 10^5 24067 CN. Approximately 24 h after infection, each mouse received i.p. 20 μCi (5 μg) of the following mAbs: groups 1 to 3, ^{188}Re-18B7; groups 4 to 6, ^{188}Re-MOPC21; groups 7 to 9, ^{188}Re-13F1; and groups 10 to 12, ^{188}Re-TEPC. At 24, 48, and 72 h after injection of radioactive mAb for ^{188}Re-18B7 and ^{188}Re-MOPC21 mAbs and at 4, 24, and 48 h for ^{188}Re-13F1 and ^{188}Re-TEPC mAbs, the groups of mice were sequentially humanely sacrificed, and their major organs were removed, weighed, and counted in a gamma counter.

In the second series of experiments, we compared the biodistribution of ^{111}In-labeled 18B7 mAb and its $F(ab')_2$ and Fab fragments in the same animal model of CN infection. Approximately 24 h after infection of six groups of three A/JCr female mice, each mouse received i.p. 20 μCi (5 μg) of the following mAbs: groups 1 to 2, ^{111}In-18B7; groups 3 to 4, ^{111}In-$F(ab')_2$; and groups 5 to 6, ^{111}In-Fab. Twenty-four and 48 h after injection of radioactive mAb, the mice were anesthetized with isoflurane and scintigraphically imaged on a gamma camera equipped with pinhole collimator (Siemens) and ICON image processing software. After imaging, the mice were humanely sacrificed and biodistribution was done as above.

Statistical analysis. The nonparametric Wilcoxon rank sum test was used to compare uptake of radioactivity in the organs in biodistribution studies. Student's t test for unpaired data was used to analyze differences in the number of colony-forming units between differently treated groups during *in vitro* radioimmunotherapy studies. Differences were considered statistically significant when P values were <0.05. The Scatchard binding and kinetics data were analyzed by linear regression (Prism software, GraphPad).

Results

Binding of ^{188}Re-18B7 and ^{188}Re-13F1 to different strains of CN. We measured pronounced differences in the abilities of

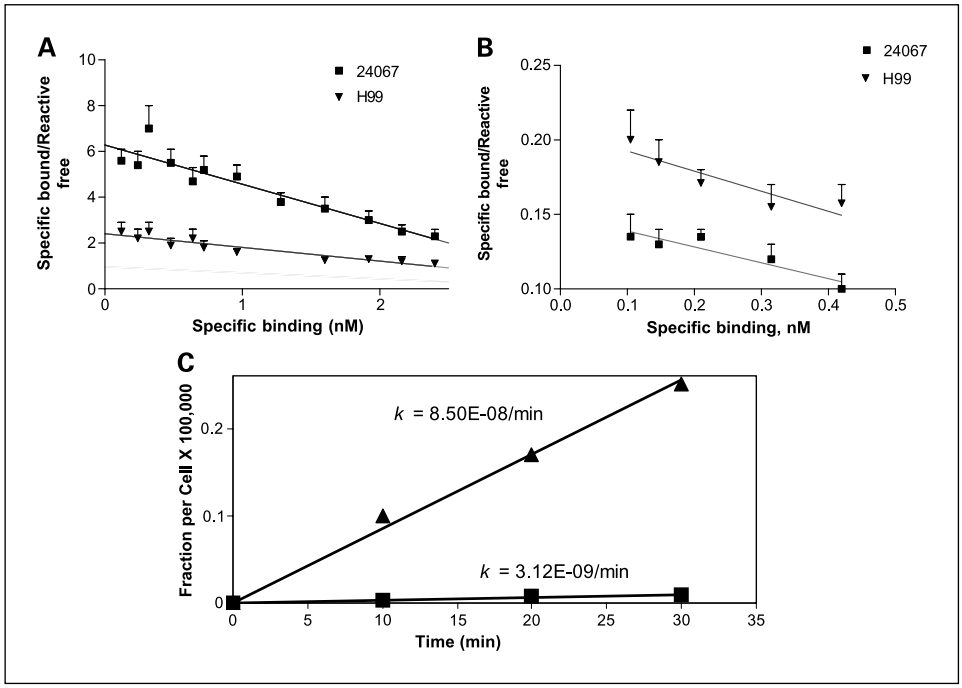

Fig. 1. Dependence of ^{188}Re-18B7 IgG1 and ^{188}Re-13F1 IgM mAbs binding to CN cells on mAb isotype and strain. *A* and *B,* Scatchard plot of ^{188}Re-18B7 and ^{188}Re-13F1 binding to 24067 and H99 CN cells. *C,* kinetics of binding of ^{188}Re-18B7 (▲) and ^{188}Re-13F1 (■) to 24067 CN cells. The binding reached saturation after 30 min and only the linear part of the binding curve is shown. The binding data are fitted to a linear function with a resulting slope of $k = 8.5 \times 10^{-8}$ min^{-1} and $k = 3.12 \times 10^{-9}$ min^{-1} for ^{188}Re-18B7 and ^{188}Re-13F1 mAbs, respectively.

^{188}Re-18B7 IgG1 and ^{188}Re-13F1 IgM to bind to both 24067 and H99 CN strains (Fig. 1A and B). The binding constants for ^{188}Re-13F1 to 24067 and H99 CN strains were approximately 31 and 7 times lower, respectively, than those for ^{188}Re-18B7 (Table 1). When the kinetics of ^{188}Re-18B7 and ^{188}Re-13F1 mAbs binding to 24067 cells was evaluated, the cellular uptake of radioactivity was linear in time up to 30 min for both mAbs (Fig. 1C), at which time saturation was reached. Linear regression analysis of the kinetics data yielded k constants, min^{-1}, of 8.5×10^{-8} and 3.12×10^{-9} for ^{188}Re-18B7 and ^{188}Re-13F1, respectively. These values were subsequently used in the cellular dosimetry calculations.

In vitro *killing of 24067 and H99 CN cells by ^{188}Re-18B7 and ^{188}Re-13F1 and cellular dosimetry results.* Treatment of 24067 and H99 CN cells with ^{188}Re-18B7 resulted in substantial killing of the cells; approximately 90% and 30%, respectively, were killed by the 1 μCi dose (Fig. 2), which delivered 55 cGy to the cells according to the cellular dosimetry calculations. In contrast, no killing with ^{188}Re-13F1 of either 24067 or H99 CN was observed in the range of activities studied (0-4.5 μCi), with the 1 μCi dose delivering 2 cGy to the treated cells.

Biodistribution of ^{188}Re-18B7 and ^{188}Re-13F1 in A/JCr mice systemically infected with 24067 CN. The animal model used in biodistribution studies used i.v. infection of A/JCr mice with CN. This model is the same as was used in the radioimmunotherapy survival experiments (2) and is suitable for the evaluation of experimental therapies because the dissemination of infection leads to rapid death in untreated mice. Figure 3A-C shows the percentage injected dose per gram (% ID/g) in CN-infected A/JCr mice injected with ^{188}Re-18B7 or isotype-matching control ^{188}Re-MOPC21. At all three time intervals (24, 48, and 72 h), the uptake of radioactivity in the liver and spleen of infected mice given ^{188}Re-18B7 was higher ($P < 0.05$) than in control group, which might be the consequence of the deposition of antibody-antigen complex (15). In contrast, the activity in the blood of mice given ^{188}Re-MOPC21 was significantly higher than in mice given ^{188}Re-18B7 ($P < 0.05$). For ^{188}Re-18B7, the highest uptake in the lungs was at 24 h (1.2% ID/g), decreasing to 0.8% and 0.4% ID/g at 48 and 72 h, respectively. The uptake in the lungs in the ^{188}Re-18B7 group was twice that of ^{188}Re-MOPC21 injected mice at 24 and 48 h and equalized at 72 h, which can be attributed to the shedding of capsular polysaccharide antigen together with the bound antibody. ^{188}Re-MOPC21 showed elevated kidney uptake at 48 h, which by 72 h became almost equal to that measured in the ^{188}Re-18B7 group. This biodistribution pattern is unlikely to be caused by instability of ^{188}Re radiolabel, as the stomach uptake, indicative of the presence of free ^{188}Re, was low at all times studied for all groups. The differences in the blood clearance between capsule-specific 18B7 IgG and the isotype-matching control are almost certainly due to the presence of polysaccharide antigen in the blood, which results in fast clearance of the specific antibody from the blood as a result of antigen-antibody complex formation and clearance by the reticuloendothelial system. This is confirmed by our previous studies that compared the

Table 1. Comparison of affinity constants and number of binding sites for 13F1 IgM and 18B7 IgG

Strain	No. binding sites per cell		Affinity constant (mol/L^{-1})	
	13F1	18B7	13F1	18B7
24067	7.7×10^5	1.1×10^6	5.4×10^7	1.7×10^9
H99	7.0×10^5	1.2×10^6	8.6×10^7	5.9×10^8

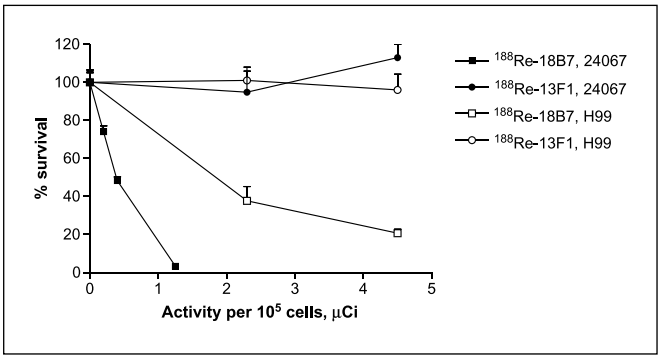

Fig. 2. *In vitro* activity of ^{188}Re-18B7 IgG1 and ^{188}Re-13F1 IgM mAbs against 24067 and H99 cells.

distribution of specific 18B7 in infection-free and infected mice to that of control MOPC21 in infected mice (2). In those studies, the blood clearance of 18B7 in infection-free animals was closer to that of MOPC21 than to 18B7 in infected mice.

The biodistribution of ^{188}Re-13F1 IgM and its isotype-matching control was done in a similar manner except that the first-time measurement was done at 4 h. The rationale for evaluating earlier time intervals for IgM than for IgG1 is that in mice IgM and IgG have serum half-life of 2 and 8 days, respectively (16). The biodistribution patterns shown in Fig. 4A-C showed that ^{188}Re-13F1 was unable to bind specifically to CN cells *in vivo*: at all time points, the uptake of ^{188}Re-13F1 in the lungs and the brain (the target organs for disseminated CN infection) was significantly ($P < 0.05$) lower for ^{188}Re-13F1 than for the control ^{188}Re-TEPC.

Biodistribution of ^{111}In-labeled 18B7 and its F(ab′)$_2$ and Fab fragments. When comparing the *in vivo* targeting of CN infection with F(ab′)$_2$ and Fab fragments versus whole antibody, the criteria for evaluating those agents would be uptake in infected and noninfected organs. *In vitro* Fab fragments manifest weaker binding to CN cells than whole mAbs or F(ab′)$_2$ because of lower valence, but *in vivo* predictions are more complicated because there are two kinds of polysaccharide antigen: on the CN cells in the infected organs and soluble polysaccharide in the blood. It is conceivable that Fab fragments bind less strongly to the soluble polysaccharide in the blood because of the lower valence yet reach infected cells in the target organs faster than whole mAb or F(ab′)$_2$ because of their smaller size. Thus, the comparative biodistribution studies were warranted. We carried out biodistribution and imaging studies with ^{111}In-labeled 18B7 and its F(ab′)$_2$ and Fab fragments (Figs. 5 and 6). At 24 h, the uptake in the lungs was 4.7% ID/g for whole ^{111}In-18B7, 1.4% ID/g for F(ab′)$_2$ fragments, and 0.2% ID/g for Fab fragments ($P = 0.03$). At 48 h, this trend changed and lung uptake of ^{111}In-F(ab′)$_2$ fragments reached 2.1% ID/g, whereas uptake of whole ^{111}In-18B7 decreased to 0.2% ID/g. This could be explained by the fact that the blood uptake of ^{111}In-F(ab′)$_2$ remained practically constant at ~1% ID/g, allowing for continuous uptake of ^{111}In-F(ab′)$_2$ into the infected lungs, whereas the blood uptake of the whole ^{111}In-18B7 fell from 2.5% ID/g at 24 h to 0.3% ID/g. Both lung and blood uptake of Fab remained low (0.2-0.3% ID/g) from 24 to 48 h. Liver uptake was several-fold higher at both 24 and 48 h for ^{111}In-18B7 (22% and 35% ID/g, respectively) and ^{111}In-F(ab′)$_2$ (20% and 10% ID/g) when compared with ^{111}In-Fab (2.5% and 2.4% ID/g), respectively. At both 24 and 48 h, the kidney uptake of F(ab′)$_2$ (12% and 12.5% ID/g) and Fab (22% and 11% ID/g) fragments was significantly higher ($P < 0.05$), due to their smaller size, when compared with whole 18B7 mAb (1% and 0.8% ID/g).

Discussion

To identify the best delivery vehicle for radioimmunotherapy of the human pathogenic fungus CN, we evaluated the pharmacokinetic and binding characteristics of capsular polysaccharide-specific antibodies with IgG1 and IgM isotypes and IgG1-derived F(ab′)$_2$ and Fab fragments.

One of the advantages of radioimmunotherapy of infection (17, 18) is that the antibodies used as delivery vehicles for radionuclides do not need to be protective as required in naked antibody therapy. In fact, the only requirement for an antibody to be a suitable reagent for radioimmunotherapy is that it binds to the targeted microbe and delivers the radionuclide to the vicinity of the microbial cell. As the binding of the organism-specific antibodies to the microbial cells in the host is the result of a complex interplay of antibody affinity, its molecular weight, and circulation time in the blood, we hypothesized that 13F1 IgM would have certain advantages as a potential carrier for the radioimmunotherapy of CN infection because of its higher valence, which might translate into higher affinity, and its shorter plasma half-life than IgG1, which will make it clear faster from the blood.

However, the binding experiments showed that the affinity constants of 13F1 for 24067 and H99 strains of CN were 31 and 7 times lower, respectively, than for 18B7. This lower binding of 13F1 IgM translated into its inability to kill CN cells during *in vitro* radioimmunotherapy experiments. In fact, the dose delivered by ^{188}Re-13F1 to CN, 2 cGy, was 28 times lower than dose delivered by the same activity of ^{188}Re-18B7. These results confirm our previous observations on the correlation between the efficacy of cell killing with the binding capacity of the mAb to the capsule (19). When given to CN-infected mice, ^{188}Re-18B7 showed specific binding to the target organs for CN infection, whereas ^{188}Re-13F1 was unable to bind specifically. High affinity of the mAb is of particular importance for the treatment of established cryptococcosis because patients with this disease often have large amounts of circulating capsular polysaccharide (cryptococcal antigen) that could interfere with radioimmunotherapy by binding radiolabeled mAb. However, in our previous studies, we found that radiolabeled 18B7 was therapeutic even in mice with serum antigen levels of ~1.9 μg/mL as determined by Latex-Crypto antigen detection system (2), which is comparable with antigen levels found in patients. The most likely explanation for this effect is that the antibody has higher affinity to capsule and tissue polysaccharide than to soluble polysaccharide. Support for this explanation comes from the competition experiments whereby very large amounts of soluble polysaccharide were needed to inhibit antibody binding to a small amount of polystyrene-absorbed polysaccharide by ELISA (20). The concentration of polysaccharide in the CN capsule is ~6 mg/mL (21), which is several thousand times higher than the concentration of soluble polysaccharide in the blood, thus providing much higher antigen density for better binding. The binding of

specific mAb to the target organ is dependent on the dose of this mAb: pretreatment of infected mice with 1 mg unlabeled 18B7 before administration of 30 μg radiolabeled 18B7 reduced uptake in the target organs 2-fold (2). The problem of high levels of circulating antigen in patients can be counteracted by using a pretargeting approach with administration of unlabeled bispecific antibodies followed by radiolabeled hapten (22).

We investigated further the influence of affinity, molecular weight, and circulation time in the blood on the biodistribution patterns of mAbs in systemic CN infection by doing comparative biodistribution experiments of ^{111}In-labeled whole 18B7 and its F(ab′)$_2$ and Fab fragments. As in the case of 13F1 IgM, which proved unsuitable for *in vivo* delivery of radionuclides because of its low affinity for the target antigen, the importance of high affinity for the target antigen again became obvious for Fab fragments. Although whole 18B7 and its F(ab′)$_2$ showed comparable uptake in the lungs, which was higher for whole ^{111}In-18B7 at 24 h after administration and for ^{111}In-F(ab′)$_2$ at 48 h, the uptake of ^{111}In-Fab in the lungs was very low at both time intervals. In cancer radioimmunotherapy, Fab fragments show significantly lower % ID/g than intact mAb despite having a smaller molecular weight as a consequence of lower affinity resulting from losing the contribution of polyvalence to avidity. For example, at 48 h after injection, the tumor % ID/g for intact mAb CC49, which binds to TAG72 antigen in human colon carcinoma xenografts, and its F(ab′)2 and Fab fragments, is 18, 13.9, and 2.7, respectively (23). The elevated kidney uptake of F(ab′)$_2$ and Fab, which is always observed in cancer radioimmunotherapy due to the lower molecular weight of the fragments in comparison with the whole mAb, also manifested itself in our study. However, it has been shown in preclinical studies and in patients that administration of positively charged amino acids effectively reduces kidney uptake of the fragments (24, 25).

It is known from cancer radioimmunotherapy (8) that the same mAb labeled with different radionuclides often displays significant differences in biodistribution. When compared with each other, ^{188}Re- and ^{111}In-labeled whole 18B7 showed comparable uptake in the infected lungs, which was highest at 24 h. Significant differences were observed in blood clearance, with ^{188}Re-18B7 clearing from the blood approximately five times faster than ^{111}In-18B7, and in liver uptake. The liver uptake of ^{111}In-labeled 18B7 was very high (35% ID/g at 48 h) compared with <2% ID/g for ^{188}Re-labeled 18B7. This can be explained by the fact that ^{111}In and other trivalent metal radiolabels tend to accumulate in the liver as a result of mAb catabolism, whereas ^{188}Re, which is attached to the mAbs directly via SH groups, is converted by mAb catabolism into perrhenate anion, which is then rapidly excreted through the kidneys. Thus, when the whole antibody is considered as a delivery vehicle for radioimmunotherapy of fungal infection, ^{188}Re seems to be a safer radioisotope than trivalent radiometals such as ^{90}Y or ^{177}Lu, which will likely show distribution patterns comparable with those of ^{111}In-labeled 18B7. Alternatively, whole antibody may be labeled with the short-lived (half-life, 46 min) α-emitter ^{213}Bi, which has already shown its efficacy and safety in radioimmunotherapy of experimental cryptococcal infection (2, 3).

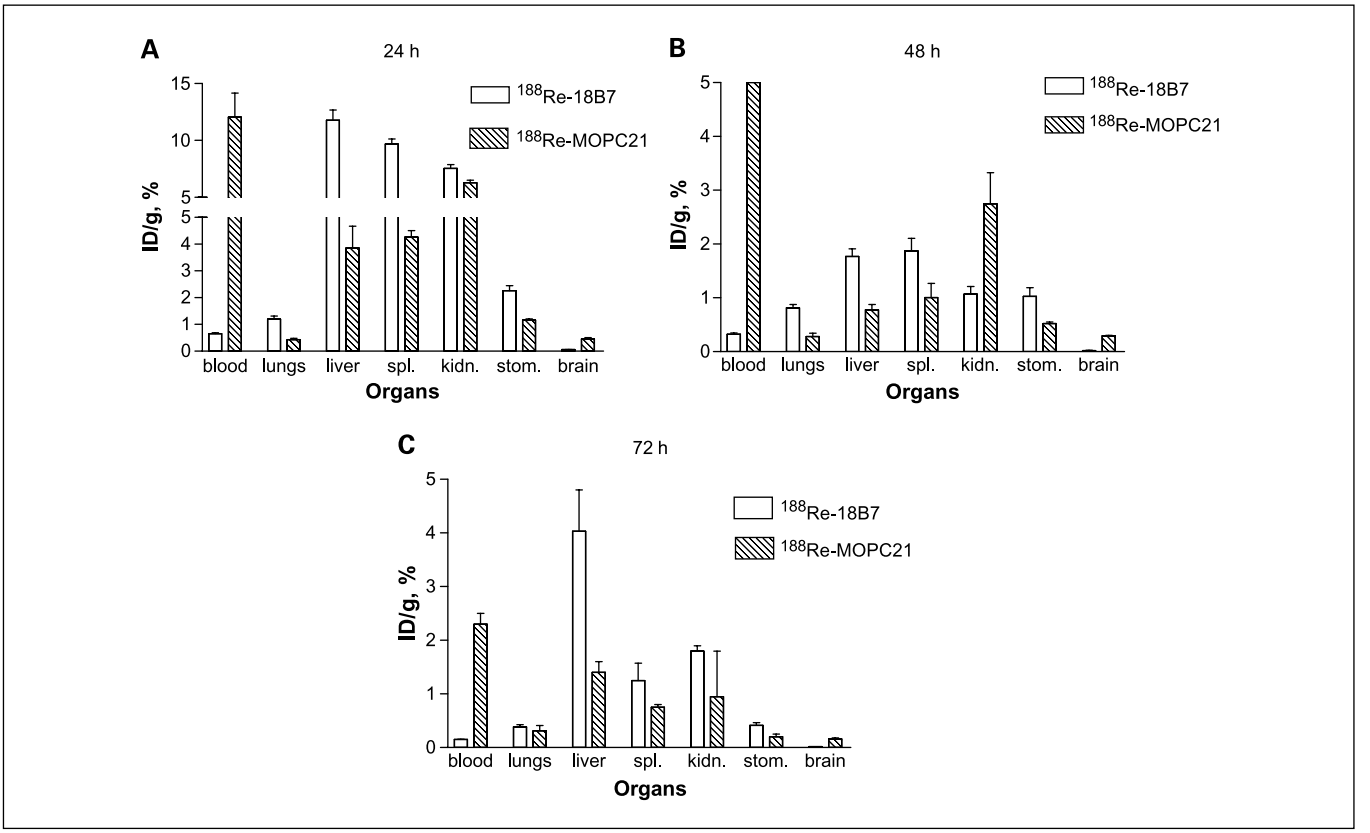

Fig. 3. Biodistribution of ^{188}Re-18B7 IgG1 and isotype-matching control ^{188}Re-MOPC21 in A/JCr mice systemically infected with 10^5 24067 CN cells 24 h before administration of radiolabeled mAbs and 24 h (*A*), 48 h (*B*), and 72 h (*C*) after administration of mAbs.

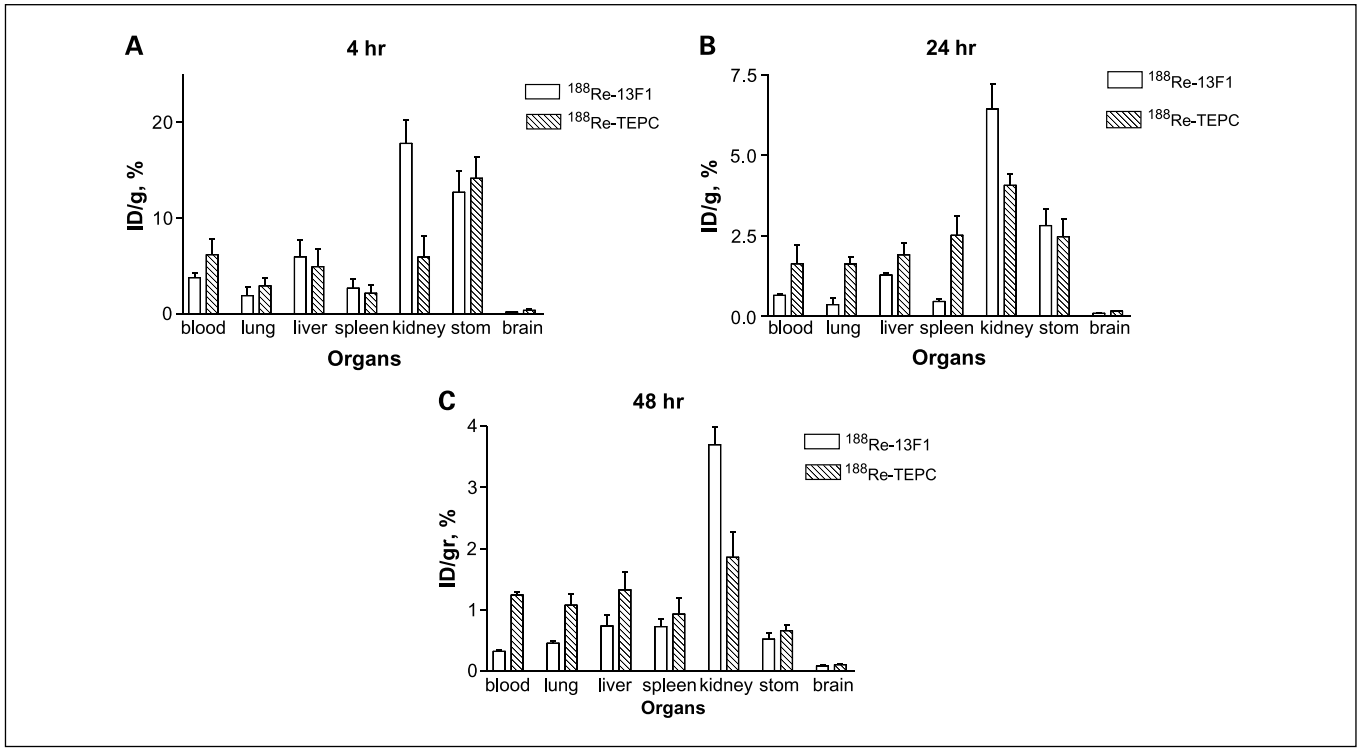

Fig. 4. Biodistribution of ^{188}Re-13F1 IgM and isotype-matching control ^{188}Re-TEPC in A/JCr mice systemically infected with 10^5 24067 CN cells 24 h before administration of radiolabeled mAbs and 4 h (*A*), 24 h (*B*), and 48 h (*C*) after administration of mAbs.

When whole ^{111}In-18B7 is compared with its ^{111}In-F(ab′)$_2$ fragments, the fragments show more stable uptake in the infected lungs and significantly less liver uptake, although even for the ^{111}In-F(ab′)$_2$ its 24- and 48-h liver uptake at 20% and 10% ID/g was approximately two and five times higher, respectively, than for ^{188}Re-labeled whole 18B7. It remains to be shown experimentally if labeling of F(ab′)$_2$ fragments with ^{188}Re will result in stable uptake in the infected organs with simultaneous reduction of the liver uptake. Although "direct" labeling of F(ab′)$_2$ fragments with ^{188}Re is impossible, chelating agents such as MAG3 could be of potential use. Labeling of F(ab′)$_2$ fragments with ^{188}Re might also offer decreased kidney toxicity because of its relatively short-half life (16.9 h) and nonresidualizing nature. ^{188}Re seems to be a safer radionuclide in terms of long-term kidney toxicity than ^{90}Y (26, 27).

In conclusion, comparative evaluation of two antibodies to cryptococcal polysaccharide with IgG and IgM isotypes and of F(ab′)$_2$ and Fab fragments of IgG mAb as potential delivery vehicles for radioimmunotherapy of cryptococcal infection strongly suggests that high affinity for the target antigen is a prerequisite for successful targeting of infection *in vivo* and that prior *in vitro* determination of affinity may predict the *in vivo* behavior of the mAbs. Based on this criteria, whole IgG mAb and its F(ab′)$_2$ fragments proved to be better choices for delivery of radionuclides than the IgM mAb used in this work or than Fab fragments. Whole IgG labeled with the

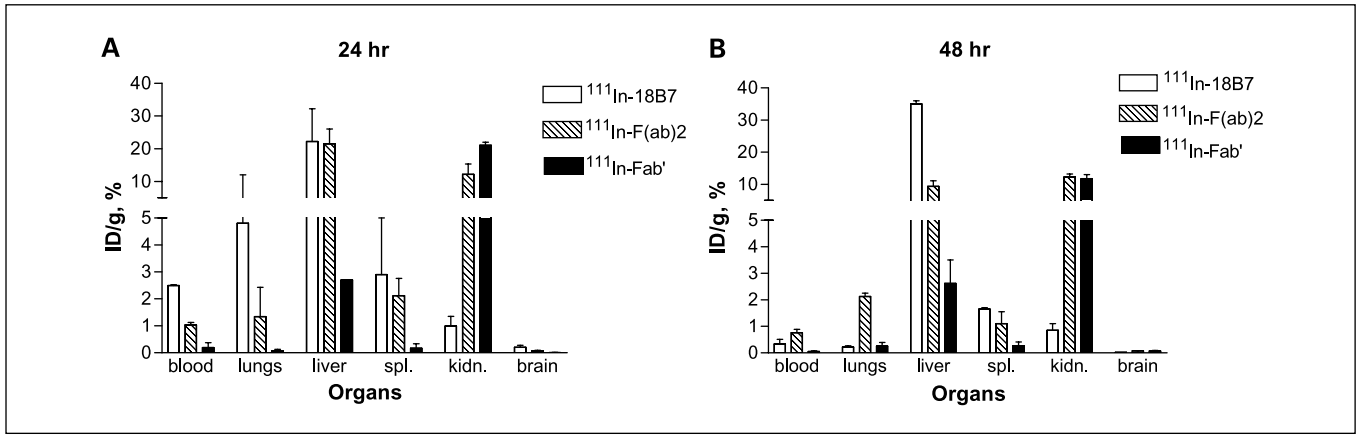

Fig. 5. Biodistribution of ^{111}In-18B7 IgG1 and its F(ab′)$_2$ and Fab fragments in A/JCr mice systemically infected with 10^5 24067 CN cells 24 h before administration of radiolabeled mAbs and 24 h (*A*) and 48 h (*B*) after administration of mAbs.

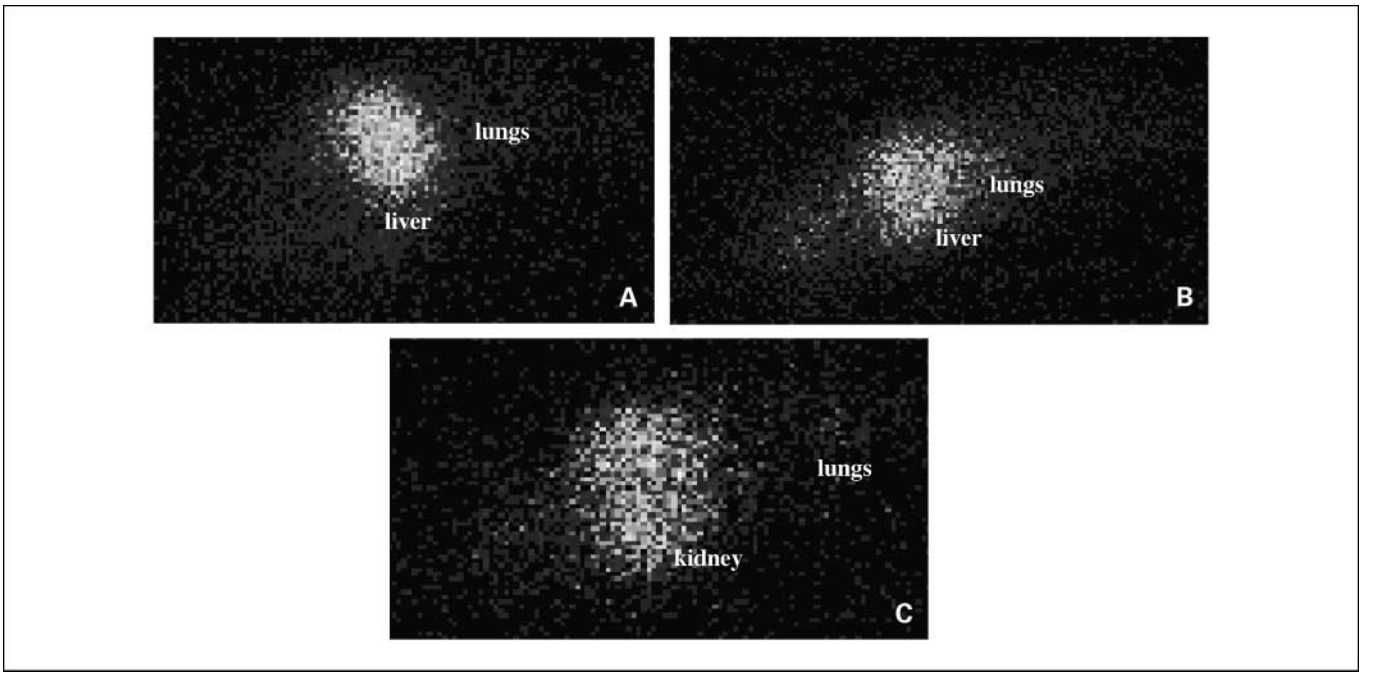

Fig. 6. Scintigraphic images of ^{111}In-18B7 IgG1 and its F(ab′)$_2$ and Fab fragments in A/JCr mice systemically infected with 10^5 24067 CN cells 24 h before administration of radiolabeled mAbs. The images were obtained 48 h after administration of mAbs: ^{111}In-18B7 (*A*), ^{111}In-F(ab′)$_2$ (*B*), and ^{111}In-Fab (*C*).

nonresidualizing radionuclide ^{188}Re also showed less uptake in the liver and kidneys than ^{111}In-labeled whole mAb or F(ab′)$_2$ fragments, which is an important safety consideration for radioimmunotherapy of infection.

Acknowledgments

We thank Dr. M.W. Brechbiel (National Cancer Institute, NIH, Bethesda, MD) for kindly providing CHXA-DTPA ligand.

References

1. Casadevall A, Dadachova E, Pirofski L. Passive antibody therapy for infectious diseases. Nat Rev Microbiol 2004;2:695–703.
2. Dadachova E, Nakouzi A, Bryan R, Casadevall A. Ionizing radiation delivered by specific antibody is therapeutic against a fungal infection. Proc Natl Acad Sci U S A 2003;100:10942–7.
3. Dadachova E, Bryan RA, Frenkel A, et al. Evaluation of acute hematological and long-term pulmonary toxicity of radioimmunotherapy of *Cryptococcus neoformans* infection in murine models. Antimicrob Agents Chemother 2004;48:1004–6.
4. Dadachova E, Howell RW, Bryan RA, Frenkel A, Nosanchuk JD, Casadevall A. Susceptibility of human pathogens *Cryptococcus neoformans* and *Histoplasma capsulatum* to γ radiation versus radioimmunotherapy with α- and β-emitting radioisotopes. J Nucl Med 2004;45:313–20.
5. Dadachova E, Burns T, Bryan RA, et al. Feasibility of radioimmunotherapy of experimental pneumococcal infection. Antimicrob Agents Chemother 2004;48:1624–9.
6. Dadachova E, Patel M, Toussi S, et al. Targeted killing of virally-infected cells by radiolabeled antibodies to viral proteins. PLoS Med 2006;3:e427.
7. Sharkey RM, Goldenberg DM. Perspectives on cancer therapy with radiolabeled monoclonal antibodies. J Nucl Med 2005;46:115–27S.
8. Milenic DE, Brady ED, Brechbiel MW. Antibody-targeted radiation cancer therapy. Nat Rev Drug Discov 2004;3:488–98.
9. Zaragoza O, Casadevall A. Experimental modulation of capsule size in *Cryptococcus neoformans*. Biol Proced Online 2004;6:10–5.
10. Casadevall A, Cleare W, Feldmesser M, et al. Characterization of a murine monoclonal antibody to *Cryptococcus neoformans* polysaccharide that is a candidate for human therapeutic studies. Antimicrob Agents Chemother 1998;42:1437–46.
11. Mukherjee J, Casadevall A, Scharff MD. Molecular characterization of the humoral responses to *Cryptococcus neoformans* infection and glucuronoxylomannan-tetanus toxoid conjugate immunization. J Exp Med 1993;177:1105–16.
12. Lowry OH, Rosebrough NJ, Farr AL, Randall RJ. Protein measurement with the Folin phenol reagent. J Biol Chem 1951;193:265–75.
13. Pippin CG, Parker TA, McMurry TJ, Brechbiel MW. Spectrophotometric method for the determination of a bifunctional DTPA ligand in DTPA-monoclonal antibody conjugates. Bioconjug Chem 1992;3:342–5.
14. Lindmo T, Boven E, Cuttitta F, Fedorko J, Bunn PA, Jr. Determination of the immunoreactive fraction of radiolabeled monoclonal antibodies by linear extrapolation to binding at infinite antigen excess. J Immunol Methods 1984;72:77–89.
15. Currie BP, Casadevall A. Estimation of the prevalence of cryptococcal infection among patients infected with the human immunodeficiency virus in New York City. Clin Infect Dis 1994;19:1029–33.
16. Vieira P, Rajewsky K. The half-lives of serum immunoglobulins in adult mice. Eur J Immunol 1988;18:313–6.
17. Dadachova E, Casadevall A. Treatment of infection with radiolabeled antibodies. Q J Nucl Med Mol Imaging 2006;50:193–204.
18. Dadachova E, Casadevall A. Antibodies as delivery vehicles for radioimmunotherapy of infectious diseases. Expert Opin Drug Deliv 2005;2:1075–84.
19. Dadachova E, Bryan RA, Apostolidis C, et al. Interaction of radiolabeled antibodies with fungal cells and components of the immune system *in vitro* and during radioimmunotherapy for experimental fungal infection. J Infect Dis 2006;193:1427–36.
20. Casadevall A, Mukherjee J, Devi SJ, Schneerson R, Robbins JB, Scharff MD. Antibodies elicited by a *Cryptococcus neoformans*-tetanus toxoid conjugate vaccine have the same specificity as those elicited in infection. J Infect Dis 1992;165:1086–93.
21. Bryan RA, Zaragoza O, Zhang T, Ortiz G, Casadevall A, Dadachova E. Radiological studies reveal radial differences in the architecture of the polysaccharide capsule of *Cryptococcus neoformans*. Eukaryotic Cell 2005;4:465–75.
22. Rossi EA, Goldenberg DM, Cardillo TM, McBride WJ, Sharkey RM, Chang CH. Stably tethered multifunctional structures of defined composition made by the dock and lock method for use in cancer targeting. Proc Natl Acad Sci U S A 2006;103:6841–6.
23. Milenic DE, Yokota T, Filpula DR, et al. Construction, binding properties, metabolism, and tumor targeting of a single-chain Fv derived from the pancarcinoma monoclonal antibody CC49. Cancer Res 1991;51:6363–71.
24. Behr TM, Sharkey RM, Juweid ME, et al. Reduction of the renal uptake of radiolabeled monoclonal antibody fragments by cationic amino acids and their derivatives. Cancer Res 1995;55:3825–34.
25. Behr TM, Becker WS, Sharkey RM, et al. Reduction of renal uptake of monoclonal antibody fragments by amino acid infusion. J Nucl Med 1996;37:829–33.
26. Dadachova E, Nosanchuk JD, Shi L, et al. Dead cells in melanoma tumors provide abundant antigen for targeted delivery of ionizing radiation by a monoclonal antibody to melanin. Proc Natl Acad Sci U S A 2004;101:14865–70.
27. Adams GP, Shaller CC, Dadachova E, et al. A single treatment of ^{90}Y-CHX-A C6.5 diabody inhibits the growth of established human tumor xenografts in immunodeficient mice. Cancer Res 2004;64:6200–6.